

# A simple method using Pyrosequencing<sup>TM</sup> to identify *de novo* SNPs in pooled DNA samples

Yeong-Shin Lin<sup>1,2,\*</sup>, Fu-Guo Robert Liu<sup>3,4</sup>, Tzi-Yuan Wang<sup>5</sup>, Cheng-Tsung Pan<sup>1</sup>, Wei-Ting Chang<sup>1</sup> and Wen-Hsiung Li<sup>4,5</sup>

<sup>1</sup>Institute of Bioinformatics and Systems Biology, <sup>2</sup>Department of Biological Science and Technology, National Chiao Tung University, Hsinchu 300, <sup>3</sup>Department of Life Science, National Central University, Taoyuan 320, Taiwan, <sup>4</sup>Department of Ecology and Evolution, University of Chicago, Chicago, IL 60637, USA and <sup>5</sup>Biodiversity Research Center, Academia Sinica, Taipei 115, Taiwan

Received May 4, 2010; Revised October 20, 2010; Accepted November 17, 2010

## ABSTRACT

A practical way to reduce the cost of surveying single-nucleotide polymorphism (SNP) in a large number of individuals is to measure the allele frequencies in pooled DNA samples. Pyrosequencing<sup>TM</sup> has been frequently used for this application because signals generated by this approach are proportional to the amount of DNA templates. The Pyrosequencing<sup>TM</sup> pyrogram is determined by the dispensing order of dNTPs, which is usually designed based on the known SNPs to avoid asynchronistic extensions of heterozygous sequences. Therefore, utilizing the pyrogram signals to identify *de novo* SNPs in DNA pools has never been undertaken. Here, in this study we developed an algorithm to address this issue. With the sequence and pyrogram of the wild-type allele known in advance, we could use the pyrogram obtained from the pooled DNA sample to predict the sequence of the unknown mutant allele (*de novo* SNP) and estimate its allele frequency. Both computational simulation and experimental Pyrosequencing<sup>TM</sup> test results suggested that our method performs well. The web interface of our method is available at <http://life.nctu.edu.tw/~yslin/PSM/>.

## INTRODUCTION

In human genomes, single-nucleotide polymorphisms (SNPs) compose the majority of genetic variation, and may, therefore, largely determine the differences among individuals. SNPs among human populations have been extensively explored in this decade (1,2). Their abundance and high potential for automation make them become a

powerful tool for identifying genetic factors, especially those contributing to complex disease susceptibility.

However, it is still expensive and time consuming to perform SNP genotyping in a large number of individuals (3). An efficient and low-cost method is important for large-scale SNP scoring. The application of current genotyping platforms for pooled DNA samples might be a practical way (3), because allele frequencies in a group of individuals could be measured using far fewer reactions (4). DNA pooling combined with whole genome analysis is usually considered as the first step to identify potential genetic markers for subsequent genotyping of individuals (5–7). Several genotyping methods suitable for measuring frequencies of SNPs in DNA pools have been proposed in the literatures (3,8).

Pyrosequencing<sup>TM</sup>, which was first described in 1988 (9), might be one of the most successful non-Sanger methods developed in the two decades (10). Instead of using 3'-modified dNTPs to terminate DNA polymerization, Pyrosequencing<sup>TM</sup> adds dNTP bases one at a time in limiting amounts to control DNA synthesis. The dNTPs are dispensed in a specific order. DNA polymerase extends the primer while the complementary dNTP is added and pauses when it encounters a noncomplementary base. The reinitiation of DNA synthesis follows the addition of the next complementary dNTP (10). As a nonfluorescence technique, Pyrosequencing<sup>TM</sup> measures the release of inorganic pyrophosphate, which is proportionally transformed into visible light by a cascade of enzymatic reactions (11,12). The generated light is recorded as a series of peaks called a pyrogram, which represents the order of complementary dNTPs and implies the underlying DNA sequence (10).

Because the light generated by the Pyrosequencing<sup>TM</sup> reactions is proportional to the amount of DNA template, this technique was frequently used to measure allelic gene expression (13,14) or allele frequency, including in tumor tissue (15), in parasites or microbial community

\*To whom correspondence should be addressed. Tel: +886 3 5712121 (ext. 56960); Fax: +886 3 5729288; Email: [yslin@faculty.nctu.edu.tw](mailto:yslin@faculty.nctu.edu.tw)

(16,17) and in DNA pools (18–22). Pyrosequencing<sup>TM</sup> has been recommended for allele frequency studies because of its high reliability in detecting variations between populations (23,24).

The ‘next-generation’ sequencing technology, including the array-based pyrosequencing (454 sequencing platform), has recently been applied for high-throughput resequencing and SNP genotyping (8,25). However, although this strategy is powerful, the expense makes it less applicable when our research interest only focuses on specific genes in specific populations. At present, most clinical laboratories use the low-throughput Pyrosequencing<sup>TM</sup> platform to identify known alleles (among organisms, strains or SNPs) (26). In this study, ‘Pyrosequencing<sup>TM</sup>’ refers to this core technology but not the array-based 454 sequencing platform. No study has applied Pyrosequencing<sup>TM</sup> for *de novo* SNP discovery (10). It is because base-calling for *de novo* SNPs is difficult and still performed manually (27). The Pyrosequencing<sup>TM</sup> pyrogram is determined by the dispensing order of dNTPs. To avoid asynchronous extensions of heterozygous sequences, the dispensing order used to be carefully designed (10). Current

sequencing software cannot detect new polymorphisms in pooled DNA samples (27), including the application of multiplex genotyping techniques (27–30).

Here, in this study, we developed an algorithm based on the normality test and dynamic programming to automatically read the pyrogram profile when unexpected mutations occurred. The performance of our method was evaluated using both computational simulation and experimental Pyrosequencing<sup>TM</sup> assays.

## MATERIALS AND METHODS

The object of our method is using a pyrogram of a pooled DNA sample to estimate the frequency of the mutant allele in the sample and predict its sequence. The sequence and pyrogram from the wild-type allele have to be known in advance. The flowchart is shown in Figure 1.

### The expected pyrogram

To illustrate our method, we used a DNA fragment, GAT CCGTTCACGTC, as an example, and assumed that this is the wild-type allele. The Pyrosequencing<sup>TM</sup> dispensing

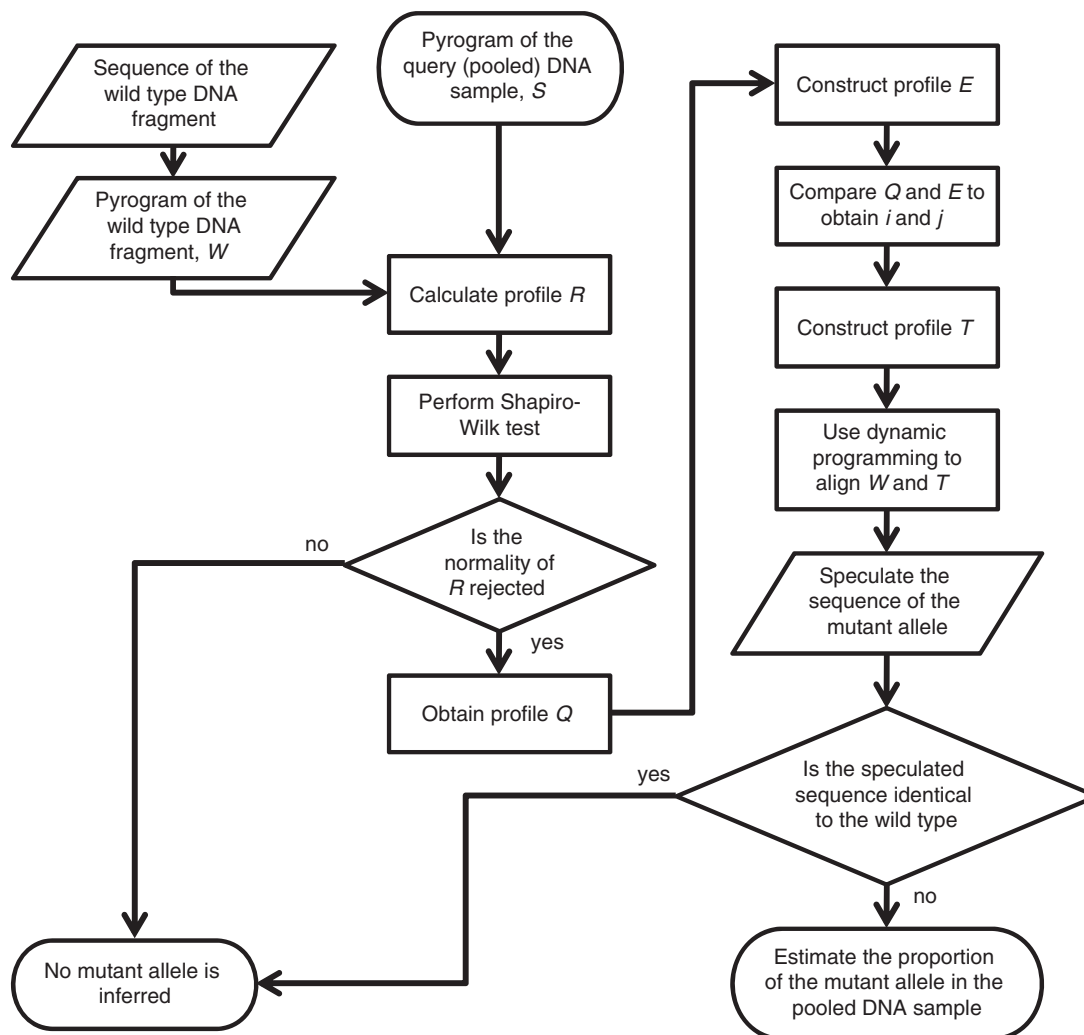
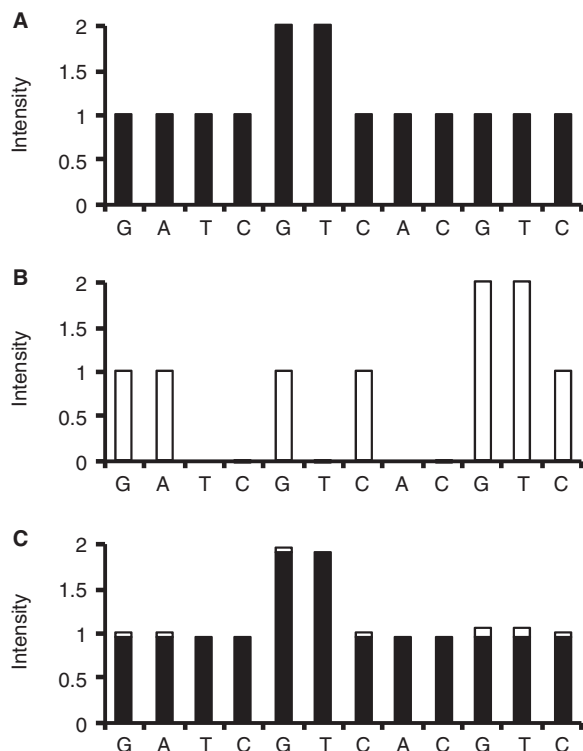


Figure 1. The flowchart of the algorithm developed in this study.



**Figure 2.** (A) The hypothetical pyrogram profile,  $W$ , for the wild-type DNA fragment, GATCGTTTACGTC; (B) the hypothetical pyrogram profile,  $M$ , for the mutant allele, GAGCGTTTACGTC; (C) the expected pyrogram profile,  $S$ , for the pooled DNA sample with 95% wild-type allele and 5% mutant allele (95% black bars + 5% white bars). All the three pyrogram profiles were simulated under the same Pyrosequencing<sup>TM</sup> dispensing order of dNTPs, GATCGTCACGTC, with  $CV = 0.5\%$ .

order of dNTPs, GATCGTCACGTC, was designated to complement this DNA fragment. Figure 2A shows the pyrogram profile,  $W$ , for this wild-type fragment. The signal intensity for the  $n$ th dispensed dNTP in  $W$  is represented as  $w_n$ . To simulate the real experiments, we defined coefficient of variation ( $CV$ ) here as the standard deviation divided by the mean, and therefore obtained  $w_n$ :

$$w_n \sim \text{Normal}[\hat{w}_n, (\hat{w}_n \times CV)^2]$$

$CV$  reflects the degree of precision for the Pyrosequencing<sup>TM</sup> experiments. In this example, we let  $CV = 0.5\%$ .

For a mutant allele with a thymine-to-guanine substitution at the third nucleotide, GAGCGTTTACGTC, asynchronous extensions would occur under the designated dispensing order of dNTPs described above. Figure 2B displays the pyrogram profile,  $M$ , for this mutant allele. Similarly, we could also obtain  $m_n$ :

$$m_n \sim \text{Normal}[\hat{m}_n, (\hat{m}_n \times CV)^2]$$

In this circumstance, for a pooled DNA sample with 95% wild-type allele and 5% mutant allele, the expected pyrogram profile,  $S$ , would be nonsynchronistic as

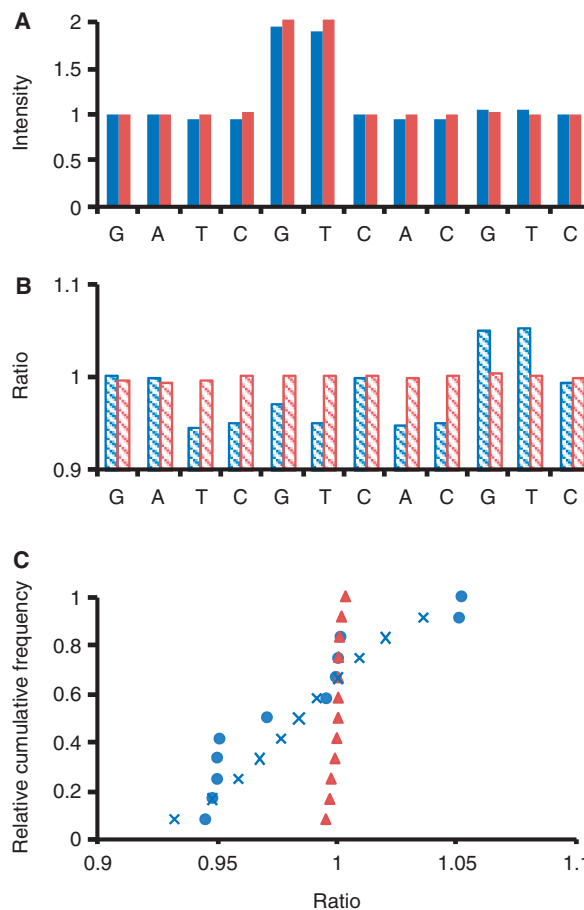


**Figure 3.** (A) The blue bars represent the pyrogram,  $S^{\text{blue}}$ , of a pooled DNA sample composed of 95% wild-type allele and 5% mutant allele as in Figure 2C. The red bars represent the pyrogram,  $S^{\text{red}}$ , of a DNA sample composed of 100% wild-type allele. The two pyrogram profiles were simulated with  $CV = 0.5\%$ . (B) The ratio profiles  $R^{\text{blue}}$  and  $R^{\text{red}}$ . (C) The relative cumulative frequencies of profiles  $Q^{\text{blue}}$  (blue circles) and  $Q^{\text{red}}$  (red triangles). The blue crosses represent the expected cumulative normal distribution,  $E^{\text{blue}}$ , which has the same mean and standard deviation as  $Q^{\text{blue}}$ . See the main text for the details.

shown in Figure 2C. The pyrogram could be predicted using the equation

$$s_n = a \times w_n + (1 - a) \times m_n$$

where  $s_n$  is the signal intensity at the  $n$ th dispensing site for  $S$ , and  $a$  represents the proportion of wild-type allele in the DNA sample. In this example,  $a = 0.95$ .

### The pyrogram to be tested

Assume that we have two unknown pooled DNA samples to be tested, and that one is actually composed of 95% wild-type allele and 5% mutant allele as in Figure 2C, while the other is composed of 100% wild-type allele as in Figure 2A. Their pyrograms,  $S^{\text{blue}}$  and  $S^{\text{red}}$ , respectively, were simulated with  $CV = 0.5\%$  and represented in Figure 3A. To distinguish  $S^{\text{blue}}$  and  $S^{\text{red}}$ , we calculated the ratio profile,  $R$ :

$$r_n^{\text{sample}} = s_n^{\text{sample}} / w_n$$

The obtained  $R^{\text{blue}}$  and  $R^{\text{red}}$  are shown in Figure 3B. Note that pyrogram  $S^{\text{blue}}$  has nonsynchronistic extensions. Therefore, when the added nucleotide during Pyrosequencing<sup>TM</sup> is not complementary to the mutant allele (for  $S^{\text{blue}}$ ,  $n = 3, 4, 6, 8$  and  $9$ ), decreased signal would be detected. For these dispensing sites,  $\hat{r}_n^{\text{blue}} = a^{\text{blue}} = 0.95$ ; while for the other sites,  $\hat{r}_n^{\text{blue}} > a^{\text{blue}}$  because  $\hat{m}_n > 0$ . As a result, the values of  $R^{\text{blue}}$  would not be normally distributed. By contrast, the distribution of the values of  $R^{\text{red}}$  should be normal, and  $\hat{r}_n^{\text{red}} = a^{\text{red}} = 1$ . We performed the Shapiro–Wilk test (31) on the normality of  $R$ , and sorted the values of  $R$  to obtain another profile,  $Q$ :

$$Q = \text{sort}(R)$$

The relative cumulative frequencies of  $Q^{\text{blue}}$  and  $Q^{\text{red}}$  are shown in Figure 3C. When the normality of  $R$  is rejected, possible nonsynchronistic extensions are implied. We therefore constructed an expected cumulative normal distribution,  $E$ , with the same mean and standard deviation as  $Q$ , and compared  $Q$  with  $E$ . In our example, the blue circles and the blue crosses represent  $Q^{\text{blue}}$  and  $E^{\text{blue}}$ , respectively (Figure 3C). As described above, for certain dispensing sites,  $\hat{r}_n^{\text{blue}} = a^{\text{blue}}$ , which corresponds to a group of the smallest values of  $Q^{\text{blue}}$ . To estimate the value of  $a^{\text{blue}}$ , we looked for a variable  $i$  that can maximize  $e_i^{\text{blue}} - q_i^{\text{blue}}$ , and then found another variable  $j$  that can minimize  $q_{j+1}^{\text{blue}} - q_{j-1}^{\text{blue}} < i$ . We then speculated that

$$a^{\text{sample}} \approx q_j^{\text{sample}}$$

In our example,  $i = 5$ ,  $j = 4$ , and  $q_4^{\text{blue}} = 0.9502$  (Figure 3C).

### The sequence of the mutant allele

Because  $a \approx q_j$ , we used  $q_j$  to construct another profile,  $T$ :

$$t_n = s_n - q_j \times w_n \approx (1 - a) \times m_n$$

The obtained  $T^{\text{blue}}$  is shown in Figure 4A.  $T$  is basically proportional to  $M$ , and could be used to infer it. However, it is inappropriate to read the sequence of the mutant allele directly from profile  $T$ , because its values are highly influenced by the coefficient of variation. Since profiles  $W$  and  $M$  could be perfectly aligned by adding gaps to  $W$  (Figure 2A and B), we used  $T$  to replace the unknown profile  $M$ , and used dynamic programming to align  $W$  and  $T$  (Figure 4). The obtained alignment was thus used to speculate the sequence of the mutant allele.

Before we perform the dynamic programming, it is worth to emphasize the *ad hoc* nature of Pyrosequencing<sup>TM</sup>:

- (i) We can only add gaps to profile  $W$ , because the dispensing order was designated to complement the wild-type DNA fragment.
- (ii) The implied sequence of the mutant allele is the set of nucleotides in  $T$  that are aligned to nucleotides in  $W$  (skipping nucleotides in  $T$  that are aligned to the added gaps). In our example, the implied sequence is GAGCGGTTC according to the alignment result in Figure 4.

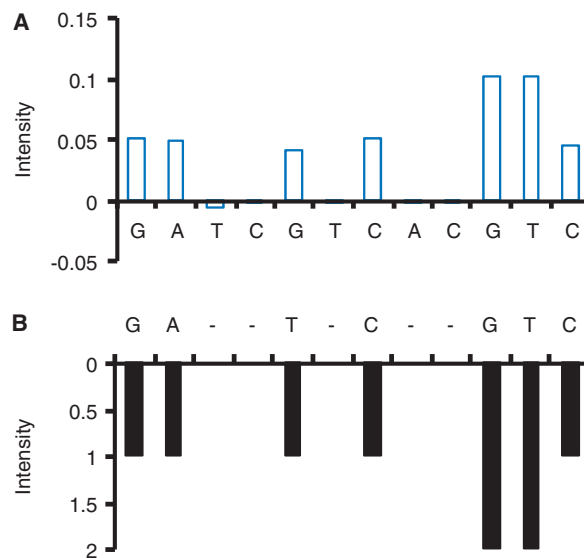


**Figure 4.** The alignment between (A) the profile  $T^{\text{blue}}$ , which is basically proportional to the unknown profile  $M$ , and (B) the profile  $W$ . See the main text for the details.

- (iii) When one gap is added to  $W$ , the corresponding nucleotide in  $T$  is suggested to be the added dNTP during Pyrosequencing<sup>TM</sup> that is noncomplementary to the mutant allele. The extension was therefore paused at that time. In our example (Figure 4), the third and fourth nucleotides in  $T$  (thymine and cytosine) are aligned to the gap in  $W$ . This alignment implies that both thymine and cytosine are not complementary to the third nucleotide of the mutant allele.
- (iv) When the gap added to  $W$  is elongated, the set of the corresponding nucleotides in  $T$  cannot include all the four dNTPs. Otherwise, all the four dNTPs are suggested to be noncomplementary to the next base of the mutant allele. In our example (Figure 4), for the first gap in  $W$ , only two dNTPs, thymine and cytosine, are included in the set of the corresponding nucleotides in  $T$ .
- (v) When the extension is reinitiated, the added dNTP (the nucleotide in  $T$  that is aligned to the current nucleotide in  $W$ ) should be complementary, and therefore cannot be one of these noncomplementary dNTPs that have appeared in the positions of  $T$  that correspond to the adjacent prior gap of  $W$ . In our example (Figure 4), when the extension is reinitiated following the first gap in  $W$ , the added complementary dNTP is guanine. This dNTP cannot be thymine or cytosine.
- (vi) For the two sites flanking the gap, the corresponding nucleotides in  $T$  cannot be the same, because the second added dNTP should be noncomplementary to the first nucleotide. In our example (Figure 4), for the two sites flanking the first gap in  $W$ , the corresponding nucleotides in  $T$  are adenine and guanine.

It should be noted that the dynamic programming is performed when the normality of profile  $R$  has been rejected, which implies possible nonsynchronistic extensions. The

nonsynchronistic extensions could result from either substitutions or insertions in the mutant allele. On the other hand, mutations are rare. We do not expect that a mutant allele with more than one *de novo* SNP in the short fragment would frequently be discovered. Therefore, the scoring scheme for the dynamic programming used in this study is defined as follows:

- The match score:  $(\bar{i} \times w_m + \bar{w} \times t_n)/2 - 2 \times |\bar{i} \times w_m - \bar{w} \times t_n|$ ;  $\bar{i}$  and  $\bar{w}$  are used to even the values of the two profiles.
- The mismatch score:  $-\infty$
- The gap penalty for profile  $W$ :  $-(\bar{w} \times t_n)$
- The gap penalty for profile  $T$ :  $-\infty$
- One mismatch site with score  $(\bar{i} \times w_m + \bar{w} \times t_n)/2 - 2 \times |\bar{i} \times w_m - \bar{w} \times t_n|$  or one gap inserted to profile  $W$  with penalty 0 is allowed.

### The estimated proportion of the wild-type allele in the pooled DNA sample

In the previous example, we assumed that the DNA quantity used for the pyrograms,  $W$  and  $S$ , are the same. However, this may not always hold. We therefore introduced another parameter,  $c$ , to represent the DNA quantity ratio:

$$s_n = c \times [a \times w_n + (1 - a) \times m_n]$$

Similar to previous sections, we speculated that  $q_j \approx ac$ . We could also obtain two equations:

$$\frac{\sum s_n - ac \sum w_n}{\sum m_n} = c \times (1 - a)$$

$$a \approx \frac{q_j}{q_j + \frac{\sum s_n - q_j}{\sum m_n} \sum w_n}$$

Although  $\sum m_n$  is unknown, we could use the alignment result to infer it. Assume that there are  $x$  elements in the pyrogram  $W$ , and  $y$  of them are aligned to profile  $T$ , which suggests that there are  $(x - y)$  gap sites in the alignment.

We could speculate that  $\sum_{n=1}^x m_n \approx \sum_{n=1}^y w_n$ . Therefore, the proportion of the wild-type allele in the pooled DNA sample was estimated as

$$a \approx \frac{q_j}{q_j + \frac{\sum_{n=1}^x s_n - q_j}{\sum_{n=1}^y w_n} \sum_{n=1}^x w_n}$$

Considering that in some cases the predicted mutant alleles may be derived from insertions, for example, an insertion at site  $z$ , we modified the equation as the following for these alleles:

$$a \approx \frac{q_j}{q_j + \frac{(\sum_{n=1}^x s_n - s_z) - q_j (\sum_{n=1}^x w_n - w_z)}{\sum_{n=1}^y w_n}}$$

### The position of the mutation site

It should be noted that the value of  $i$ , which maximizes  $e_i - q_i$ , depends on the position of the mutant site. When

the mutant site is located close to the end of the pyrogram, the value of  $i$  (and the proportion of  $i$  to  $x$ ) would be small. In this circumstance, the normality of profile  $R$  may not be rejected because the signals of nonsynchronistic extensions are likely to be diluted. To overcome this problem, we tested the normality in a sliding window. The window size was designated as 30 in our study. As the window slides, if the normality is rejected for a certain window, we would use this window and its downstream pyrogram to derive the profile  $Q$ , and variables  $i$ ,  $j$  and  $q_j$ .

### Performance testing by computational simulation

We utilized simulation tests to evaluate the performance of our algorithm. The tested DNA fragments are listed below:

ACACCAAGTCGTGTTACAGTGGCTAAGTTCCG  
CCAGCCTCAC—the wild-type allele;  
ACGCCAAGTCGTGTTACAGTGGCTAAGTTCCG  
CCAGCCTCAC—the mutant allele with an adenosine-to-guanine substitution at the third nucleotide;  
ACAGCCAAGTCGTGTTACAGTGGCTAAGTTCC  
GCCAGCCTCAC—the mutant allele with a guanine inserted between the third and fourth nucleotides;  
ACACCAAGTCGTGTTACAGTGGCTAAGTTCCG  
CCATCCTCAC—the mutant allele with a guanine-to-thymine substitution at the 37th nucleotide; and  
ACACCAAGTCGTGTTACAGTGGCTAAGTTCCG  
CCAGCCACAC—the mutant allele with a thymine-to-adenosine substitution at the 40th nucleotide.

The Pyrosequencing<sup>TM</sup> dispensing order of dNTPs, ACA CAGTCGTGTCACAGTGCTAGTCGCAGCTCAC, was designated to complement the wild-type allele. The tested DNA pools contained 0%, 1%, 2%, 4%, 8%, 16%, 32% or 64% mutant allele. The pyrograms of these pooled DNA samples were simulated with different degrees of experimental precision ( $CV = 0.01\%$ ,  $0.02\%$ ,  $0.04\%$ ,  $0.08\%$ ,  $0.16\%$ ,  $0.32\%$ ,  $0.64\%$ ,  $1.28\%$ ,  $2.56\%$ ,  $5.12\%$ ,  $10.24\%$  and  $20.48\%$ ). When the normality of profile  $R$  was rejected ( $P < 0.01$ , Shapiro–Wilk test), dynamic programming was performed to speculate the sequence of the mutant allele; otherwise, no mutant allele was inferred. If the speculated sequence of the mutant allele was identical to the wild-type (except for the last couple nucleotides, which may not be well aligned when  $CV$  is high), no mutant allele was inferred, either. The simulation tests were repeated 10 000 times. If our method positively identified a mutant allele, we estimated the proportion of the wild-type allele in the DNA pool, despite whether the speculated sequence is correct or not. The mean and standard deviation of the estimated proportion of the wild-type allele in the DNA pool were thus calculated.

### Performance testing by real Pyrosequencing<sup>TM</sup>

We first used a real Pyrosequencing<sup>TM</sup> assay as an example. The DNA samples were obtained from mitochondrial cytochrome *b* gene of *Pseudorasbora parva* specimens. The test region was amplified using a specific primer pair: forward – GTGTGAAGTTGTCGGGGT

CT; reverse – CCGCAACGGTTATCCATCTT. The Biotin tag was attached on the reverse primer. Polymerase chain reaction (PCR) was conducted using *Taq* DNA polymerase (Biokit Biotechnology, Taiwan) in a reaction mixture containing 25 ng of DNA template, 100 nM of biotin-labeled reverse primer and 100 nM of the forward primer. The PCR cycling program consisted of denaturation at 94°C for 1 min; followed by 40 cycles of denaturation at 94°C for 20 s, annealing at 60°C for 20 s, and extension at 72°C for 15 s; and the final extension at 72°C for 7 min. PCR products were purified with PCR clean-up kit (Biokit Biotechnology). The pooled DNA sample contained 90% PCR products of one allele (CCT AACAGGTTAGGGGAAAATAGCGCTAGAGATGT AAGGGCCAACAATATTAATACAAAGCCAAGAA GGTCTTTGT for the first 76 bases) as the wild-type and 10% PCR products of another allele with a cytosine-to-thymine substitution at the 6th nucleotide (CCTAA TAGGTTAGGGGAAAATAGCGCT for the first 27 bases) as the mutant allele. The concentrations of the DNA samples were measured using ND-1000 (Nanodrop Technologies, Wilmington, DE, USA) at OD<sub>260</sub>. Biotinylated single-stranded DNA in 40 µl PCR solution containing 600 ng pooled DNA samples and the forward primer were used for the Pyrosequencing<sup>TM</sup> reaction, which was performed in accordance with the manufacturer's instructions (www.pyrosequencing.com) using Pyro Gold SQA Reagents (Qiagen, Hilden, Germany) by model PyroMark ID (Biotage AB, Uppsala, Sweden).

To reveal how practical our method is in real experiments, another large-scale Pyrosequencing<sup>TM</sup> assay was conducted. A partial region of YBR114W gene was amplified for both the two yeast strains, BY4741 (BY, a laboratory strain) and RM11-1a (RM, a wild strain) with a specific primer pair: forward – AAGCAAAGTATTGT TAGCCGTCTA; reverse – ATCCAGCTCTTTTCAATC TCC. The Biotin tag was also attached on the reverse primer. Another forward sequencing primer, GCCGTCT AACATGAGT, was used for the Pyrosequencing<sup>TM</sup> reaction. The sequences to be read in the Pyrosequencing<sup>TM</sup> reactions for BY and RM are GGCA AGTGGCAATCATCAACGAAAATCGAAGCACT<sup>-</sup> and GGTAAGTGGCAATCATCAACGAAAATCGAA GCACT<sup>-</sup>, respectively. A cytosine-to-thymine substitution is at the third nucleotide. We prepared the wild-type sample using 100% RM and the unknown pooled DNA sample using 90% RM + 10% BY. Both samples were repeated 12 times. One hundred and forty-four sample pairs could therefore be obtained. The derived pyrograms are represented in Supplementary Data.

## RESULTS AND DISCUSSION

The simulation results are listed in Tables 1 and 2. When the variation in the pyrogram signals was limited (the level of precision was high), e.g.  $CV < 0.1\%$ , in most cases, our method could perfectly predict the DNA sequence of the mutant allele, either a substitution or an insertion, and its proportion in the DNA pools. However, when the signal variation was high (the level of precision was low), the

prediction power of our method decreased with the proportion of the mutant allele in the DNA pool. For example, in Table 1, when  $CV = 2.56\%$ , we precisely estimated the proportion of the mutant allele (with one substitution at the third nucleotide) in the DNA pool while its real proportion is 16% (estimated as  $16.00 \pm 2.87\%$ ); however, when the real proportion decreased to 1%, our method tended to overestimate its value ( $3.32 \pm 2.69\%$ ). Similarly, in Table 2, when  $CV = 2.56\%$ , we accurately predicted the sequence of the mutant allele (with one substitution at the third nucleotide) in all the 10000 repeats while its proportion in the DNA pool is 32%; however, when the real proportion decreased to 1%, we only identified a mutant allele 507 times from the 10000 repeats, and only nine of them had their sequence accurately predicted. Note that the standard deviation of the estimated allele frequencies also increased with  $CV$  (Table 1). These results suggested that the performance of our method is highly correlated to the variation in the pyrogram signals (the level of experimental precision) and the proportion of the mutant allele in the DNA pool. We also examined the possibility that we inaccurately predicted the existence of a mutant allele in a DNA pool consisting of 100% wild-type allele. The false positive ratio was  $< 5\%$  when  $CV < 5\%$  (Table 2). Moreover, even in these cases, the estimated proportion of the wild-type allele in the DNA pool did not deviate from 100% too much when the signal variation was limited (Table 1).

Since sufficient signals of nonsynchronistic extensions are crucial for our algorithm, one might argue that it would be difficult to identify a mutant allele if its mutant site was located close to the end of the pyrogram. Our simulation revealed that, when the substitution was located at the 40th nucleotide, our algorithm almost did not have the identification power (Tables 1 and 2) because the generated profile  $R$  had only two sites with  $\hat{r}_n = a$ . In this circumstance, it was difficult to obtain a reasonable  $i$ , and also the variables  $j$ , and  $q_j$ . We therefore were unable to correctly align the profiles and predict the mutant sequence. However, when the substitution was located at the 37th nucleotide instead (with four sites  $\hat{r}_n = a$ ), our algorithm performed almost the same as when the substitution was located at the third nucleotide (Tables 1 and 2). This result suggested that our method should have a wide application.

We also performed real Pyrosequencing<sup>TM</sup> assays to reveal how our algorithm works. In our first example (Figure 5), the mitochondrial cytochrome *b* gene of *P. parva* was used. Figure 5A and B display the pyrograms for the wild-type DNA fragment and the pooled DNA sample containing 10% mutant allele, respectively. Although it might not be easy to distinguish these two pyrograms by eyes, our algorithm successfully identified the sequence of the mutant allele (Figure 5D and E), and estimated its proportion in the DNA pool as 12.0%. The deviation of this estimated value is likely due to the variation in the pyrogram signals. This variation could be revealed from the constructed profile  $T$  in Figure 5D. According to the Pyrosequencing<sup>TM</sup> dispensing order of dNTPs and the sequence of the mutant allele, the

Table 1. The estimated proportion of the wild-type allele in the DNA pool under various simulated conditions  
CV The mean  $\pm$  standard deviation of the estimated proportion of the wild-type allele in the DNA pool

	$a = 1.00$	$a = 0.99$	$a = 0.98$	$a = 0.96$	$a = 0.92$	$a = 0.84$	$a = 0.68$	$a = 0.36$
<b>Mutant allele with an adenosine-to-guanine substitution at the third nucleotide</b>								
0.01%	0.9999 $\pm$ 0.0001	0.9900 $\pm$ 0.0001	0.9800 $\pm$ 0.0001	0.9600 $\pm$ 0.0001	0.9200 $\pm$ 0.0001	0.8400 $\pm$ 0.0001	0.6800 $\pm$ 0.0001	0.3600 $\pm$ 0.0001
0.02%	0.9997 $\pm$ 0.0002	0.9900 $\pm$ 0.0003	0.9800 $\pm$ 0.0003	0.9600 $\pm$ 0.0003	0.9200 $\pm$ 0.0002	0.8400 $\pm$ 0.0002	0.6800 $\pm$ 0.0002	0.3600 $\pm$ 0.0001
0.04%	0.9994 $\pm$ 0.0004	0.9900 $\pm$ 0.0006	0.9800 $\pm$ 0.0006	0.9600 $\pm$ 0.0005	0.9200 $\pm$ 0.0005	0.8400 $\pm$ 0.0004	0.6800 $\pm$ 0.0003	0.3600 $\pm$ 0.0002
0.08%	0.9988 $\pm$ 0.0009	0.9900 $\pm$ 0.0011	0.9800 $\pm$ 0.0011	0.9600 $\pm$ 0.0011	0.9200 $\pm$ 0.0010	0.8400 $\pm$ 0.0009	0.6800 $\pm$ 0.0007	0.3600 $\pm$ 0.0004
0.16%	0.9977 $\pm$ 0.0018	0.9899 $\pm$ 0.0024	0.9800 $\pm$ 0.0022	0.9600 $\pm$ 0.0021	0.9200 $\pm$ 0.0020	0.8400 $\pm$ 0.0018	0.6800 $\pm$ 0.0013	0.3600 $\pm$ 0.0008
0.32%	0.9954 $\pm$ 0.0036	0.9898 $\pm$ 0.0059	0.9798 $\pm$ 0.0049	0.9599 $\pm$ 0.0042	0.9200 $\pm$ 0.0040	0.8400 $\pm$ 0.0035	0.6800 $\pm$ 0.0026	0.3600 $\pm$ 0.0017
0.64%	0.9910 $\pm$ 0.0070	0.9881 $\pm$ 0.0086	0.9796 $\pm$ 0.0117	0.9598 $\pm$ 0.0092	0.9199 $\pm$ 0.0079	0.8399 $\pm$ 0.0069	0.6799 $\pm$ 0.0052	0.3600 $\pm$ 0.0033
1.28%	0.9822 $\pm$ 0.0138	0.9830 $\pm$ 0.0142	0.9763 $\pm$ 0.0170	0.9593 $\pm$ 0.0229	0.9196 $\pm$ 0.0167	0.8401 $\pm$ 0.0138	0.6799 $\pm$ 0.0105	0.3599 $\pm$ 0.0066
2.56%	0.9654 $\pm$ 0.0275	0.9668 $\pm$ 0.0269	0.9652 $\pm$ 0.0283	0.9541 $\pm$ 0.0340	0.9206 $\pm$ 0.0449	0.8400 $\pm$ 0.0287	0.6802 $\pm$ 0.0213	0.3599 $\pm$ 0.0132
5.12%	0.9352 $\pm$ 0.0546	0.9336 $\pm$ 0.0528	0.9363 $\pm$ 0.0532	0.9335 $\pm$ 0.0565	0.9111 $\pm$ 0.0675	0.8437 $\pm$ 0.0837	0.6801 $\pm$ 0.0457	0.3597 $\pm$ 0.0267
10.24%	0.8807 $\pm$ 0.1069	0.8871 $\pm$ 0.1073	0.8862 $\pm$ 0.1071	0.8848 $\pm$ 0.1076	0.8784 $\pm$ 0.1126	0.8395 $\pm$ 0.1387	0.6919 $\pm$ 0.1505	0.3603 $\pm$ 0.0526
20.48%	0.8315 $\pm$ 0.2466	0.8314 $\pm$ 0.2546	0.8280 $\pm$ 0.2627	0.8282 $\pm$ 0.2467	0.8283 $\pm$ 0.2743	0.8130 $\pm$ 0.2543	0.7490 $\pm$ 0.3271	0.3464 $\pm$ 4.3826
<b>Mutant allele with a guanine inserted between the third and fourth nucleotides</b>								
0.01%	0.9999 $\pm$ 0.0001	0.9900 $\pm$ 0.0001	0.9800 $\pm$ 0.0001	0.9600 $\pm$ 0.0001	0.9200 $\pm$ 0.0001	0.8400 $\pm$ 0.0001	0.6800 $\pm$ 0.0001	0.3600 $\pm$ 0.0001
0.02%	0.9998 $\pm$ 0.0002	0.9900 $\pm$ 0.0003	0.9800 $\pm$ 0.0003	0.9600 $\pm$ 0.0003	0.9200 $\pm$ 0.0002	0.8400 $\pm$ 0.0002	0.6800 $\pm$ 0.0002	0.3600 $\pm$ 0.0001
0.04%	0.9997 $\pm$ 0.0005	0.9900 $\pm$ 0.0005	0.9800 $\pm$ 0.0005	0.9600 $\pm$ 0.0005	0.9200 $\pm$ 0.0005	0.8400 $\pm$ 0.0004	0.6800 $\pm$ 0.0003	0.3600 $\pm$ 0.0002
0.08%	0.9994 $\pm$ 0.0010	0.9900 $\pm$ 0.0011	0.9800 $\pm$ 0.0010	0.9600 $\pm$ 0.0010	0.9200 $\pm$ 0.0010	0.8400 $\pm$ 0.0008	0.6800 $\pm$ 0.0006	0.3600 $\pm$ 0.0004
0.16%	0.9986 $\pm$ 0.0019	0.9899 $\pm$ 0.0023	0.9801 $\pm$ 0.0021	0.9600 $\pm$ 0.0020	0.9200 $\pm$ 0.0019	0.8400 $\pm$ 0.0017	0.6800 $\pm$ 0.0013	0.3600 $\pm$ 0.0008
0.32%	0.9974 $\pm$ 0.0037	0.9903 $\pm$ 0.0059	0.9798 $\pm$ 0.0044	0.9601 $\pm$ 0.0041	0.9200 $\pm$ 0.0038	0.8399 $\pm$ 0.0034	0.6800 $\pm$ 0.0026	0.3600 $\pm$ 0.0016
0.64%	0.9947 $\pm$ 0.0075	0.9888 $\pm$ 0.0089	0.9811 $\pm$ 0.0115	0.9597 $\pm$ 0.0093	0.9199 $\pm$ 0.0076	0.8399 $\pm$ 0.0067	0.6800 $\pm$ 0.0051	0.3600 $\pm$ 0.0032
1.28%	0.9892 $\pm$ 0.0157	0.9867 $\pm$ 0.0159	0.9789 $\pm$ 0.0176	0.9615 $\pm$ 0.0220	0.9195 $\pm$ 0.0169	0.8400 $\pm$ 0.0134	0.6799 $\pm$ 0.0102	0.3600 $\pm$ 0.0063
2.56%	0.9808 $\pm$ 0.0296	0.9756 $\pm$ 0.0289	0.9697 $\pm$ 0.0284	0.9580 $\pm$ 0.0342	0.9251 $\pm$ 0.0453	0.8393 $\pm$ 0.0291	0.6797 $\pm$ 0.0205	0.3601 $\pm$ 0.0128
5.12%	0.9502 $\pm$ 0.0547	0.9538 $\pm$ 0.0560	0.9508 $\pm$ 0.0544	0.9413 $\pm$ 0.0606	0.9254 $\pm$ 0.0773	0.8492 $\pm$ 0.0863	0.6801 $\pm$ 0.0477	0.3599 $\pm$ 0.0257
10.24%	0.9170 $\pm$ 0.1206	0.9188 $\pm$ 0.1193	0.9223 $\pm$ 0.1269	0.9144 $\pm$ 0.1222	0.9006 $\pm$ 0.1369	0.8573 $\pm$ 0.1565	0.7043 $\pm$ 0.1812	0.3556 $\pm$ 0.5902
20.48%	0.8898 $\pm$ 0.3129	0.8969 $\pm$ 0.3699	0.9005 $\pm$ 0.5321	0.8804 $\pm$ 0.3253	0.8773 $\pm$ 0.3134	0.8779 $\pm$ 0.5953	0.7953 $\pm$ 1.6143	0.3580 $\pm$ 3.9309
<b>Mutant allele with a thymine-to-thymine substitution at the 37th nucleotide</b>								
0.01%	0.9999 $\pm$ 0.0001	0.9900 $\pm$ 0.0001	0.9800 $\pm$ 0.0001	0.9600 $\pm$ 0.0001	0.9200 $\pm$ 0.0001	0.8400 $\pm$ 0.0001	0.6800 $\pm$ 0.0001	0.3600 $\pm$ 0.0000
0.02%	0.9998 $\pm$ 0.0002	0.9900 $\pm$ 0.0002	0.9800 $\pm$ 0.0002	0.9600 $\pm$ 0.0002	0.9200 $\pm$ 0.0002	0.8400 $\pm$ 0.0002	0.6800 $\pm$ 0.0001	0.3600 $\pm$ 0.0001
0.04%	0.9997 $\pm$ 0.0005	0.9900 $\pm$ 0.0004	0.9800 $\pm$ 0.0004	0.9600 $\pm$ 0.0003	0.9200 $\pm$ 0.0003	0.8400 $\pm$ 0.0003	0.6800 $\pm$ 0.0003	0.3600 $\pm$ 0.0002
0.08%	0.9993 $\pm$ 0.0009	0.9900 $\pm$ 0.0007	0.9800 $\pm$ 0.0007	0.9600 $\pm$ 0.0007	0.9200 $\pm$ 0.0007	0.8400 $\pm$ 0.0006	0.6800 $\pm$ 0.0005	0.3600 $\pm$ 0.0004
0.16%	0.9985 $\pm$ 0.0018	0.9900 $\pm$ 0.0015	0.9800 $\pm$ 0.0015	0.9600 $\pm$ 0.0014	0.9200 $\pm$ 0.0014	0.8400 $\pm$ 0.0012	0.6800 $\pm$ 0.0010	0.3600 $\pm$ 0.0008
0.32%	0.9975 $\pm$ 0.0037	0.9900 $\pm$ 0.0047	0.9800 $\pm$ 0.0031	0.9601 $\pm$ 0.0028	0.9200 $\pm$ 0.0027	0.8400 $\pm$ 0.0024	0.6800 $\pm$ 0.0020	0.3600 $\pm$ 0.0016
0.64%	0.9948 $\pm$ 0.0076	0.9916 $\pm$ 0.0085	0.9803 $\pm$ 0.0096	0.9598 $\pm$ 0.0058	0.9201 $\pm$ 0.0054	0.8400 $\pm$ 0.0049	0.6801 $\pm$ 0.0041	0.3600 $\pm$ 0.0032
1.28%	0.9885 $\pm$ 0.0144	0.9881 $\pm$ 0.0146	0.9853 $\pm$ 0.0170	0.9595 $\pm$ 0.0172	0.9198 $\pm$ 0.0111	0.8401 $\pm$ 0.0098	0.6799 $\pm$ 0.0083	0.3600 $\pm$ 0.0065
2.56%	0.9774 $\pm$ 0.0296	0.9774 $\pm$ 0.0276	0.9741 $\pm$ 0.0277	0.9700 $\pm$ 0.0342	0.9173 $\pm$ 0.0304	0.8395 $\pm$ 0.0198	0.6799 $\pm$ 0.0164	0.3601 $\pm$ 0.0129
5.12%	0.9531 $\pm$ 0.0535	0.9590 $\pm$ 0.0577	0.9552 $\pm$ 0.0542	0.9533 $\pm$ 0.0567	0.9367 $\pm$ 0.0640	0.8463 $\pm$ 0.0670	0.6798 $\pm$ 0.0329	0.3600 $\pm$ 0.0255
10.24%	0.9108 $\pm$ 0.1205	0.9112 $\pm$ 0.1175	0.9142 $\pm$ 0.1161	0.9162 $\pm$ 0.1199	0.9059 $\pm$ 0.1164	0.8901 $\pm$ 0.1305	0.6954 $\pm$ 0.1258	0.3595 $\pm$ 0.0516
20.48%	0.8806 $\pm$ 0.3044	0.8952 $\pm$ 0.3788	0.8890 $\pm$ 0.3120	0.8957 $\pm$ 0.3257	0.8863 $\pm$ 0.3063	0.8816 $\pm$ 0.3128	0.8718 $\pm$ 0.3127	0.5032 $\pm$ 0.4090
<b>Mutant allele with a thymine-to-adenosine substitution at the 40th nucleotide</b>								
0.01%	0.9999 $\pm$ 0.0001	1.0008 $\pm$ 0.0003	1.0015 $\pm$ 0.0005	1.0031 $\pm$ 0.0011	1.0061 $\pm$ 0.0021	1.0124 $\pm$ 0.0043	1.0250 $\pm$ 0.0088	1.0518 $\pm$ 0.0187
0.02%	0.9998 $\pm$ 0.0002	1.0008 $\pm$ 0.0003	1.0015 $\pm$ 0.0006	1.0030 $\pm$ 0.0011	1.0061 $\pm$ 0.0021	1.0123 $\pm$ 0.0043	1.0248 $\pm$ 0.0088	1.0511 $\pm$ 0.0185
0.04%	0.9997 $\pm$ 0.0005	1.0008 $\pm$ 0.0006	1.0015 $\pm$ 0.0007	1.0031 $\pm$ 0.0012	1.0061 $\pm$ 0.0022	1.0124 $\pm$ 0.0044	1.0250 $\pm$ 0.0088	1.0515 $\pm$ 0.0186
0.08%	0.9992 $\pm$ 0.0009	1.0011 $\pm$ 0.0013	1.0016 $\pm$ 0.0012	1.0031 $\pm$ 0.0014	1.0061 $\pm$ 0.0023	1.0124 $\pm$ 0.0044	1.0251 $\pm$ 0.0089	1.0515 $\pm$ 0.0187
0.16%	0.9985 $\pm$ 0.0018	1.0003 $\pm$ 0.0035	1.0022 $\pm$ 0.0025	1.0033 $\pm$ 0.0025	1.0062 $\pm$ 0.0027	1.0124 $\pm$ 0.0047	1.0252 $\pm$ 0.0091	1.0516 $\pm$ 0.0188
0.32%	0.9974 $\pm$ 0.0038	0.9974 $\pm$ 0.0061	1.0004 $\pm$ 0.0070	1.0044 $\pm$ 0.0051	1.0066 $\pm$ 0.0047	1.0124 $\pm$ 0.0055	1.0250 $\pm$ 0.0095	1.0517 $\pm$ 0.0191
0.64%	0.9947 $\pm$ 0.0073	0.9939 $\pm$ 0.0090	0.9948 $\pm$ 0.0124	1.0010 $\pm$ 0.0139	1.0089 $\pm$ 0.0098	1.0132 $\pm$ 0.0093	1.0249 $\pm$ 0.0109	1.0513 $\pm$ 0.0201
1.28%	0.9881 $\pm$ 0.0141	0.9873 $\pm$ 0.0154	0.9869 $\pm$ 0.0187	0.9908 $\pm$ 0.0246	1.0037 $\pm$ 0.0269	1.0178 $\pm$ 0.0199	1.0263 $\pm$ 0.0177	1.0517 $\pm$ 0.0233
2.56%	0.9757 $\pm$ 0.0298	0.9751 $\pm$ 0.0299	0.9751 $\pm$ 0.0283	0.9710 $\pm$ 0.0331	0.9808 $\pm$ 0.0487	1.0100 $\pm$ 0.0497	1.0358 $\pm$ 0.0380	1.0547 $\pm$ 0.0376
5.12%	0.9578 $\pm$ 0.0584	0.9507 $\pm$ 0.0559	0.9510 $\pm$ 0.0544	0.9506 $\pm$ 0.0580	0.9489 $\pm$ 0.0625	0.9658 $\pm$ 0.0896	1.0293 $\pm$ 0.0910	1.0742 $\pm$ 0.0820
10.24%	0.9179 $\pm$ 0.1261	0.9043 $\pm$ 0.1042	0.9236 $\pm$ 0.1298	0.9050 $\pm$ 0.1095	0.9180 $\pm$ 0.1220	0.9013 $\pm$ 0.1217	0.9420 $\pm$ 0.1700	1.0736 $\pm$ 0.1752
20.48%	0.8923 $\pm$ 0.3268	0.8918 $\pm$ 0.3525	0.8920 $\pm$ 0.3403	0.8880 $\pm$ 0.3378	0.8931 $\pm$ 0.3038	0.8825 $\pm$ 0.2935	0.8715 $\pm$ 0.2986	0.9362 $\pm$ 0.3909

$\sigma$  indicates the real proportion of the wild-type allele in the DNA pool.

**Table 2.** The accuracy of the mutant allele identification in the DNA pool under various simulated conditions

CV	True positive/positive							
	$a = 1.00$	$a = 0.99$	$a = 0.98$	$a = 0.96$	$a = 0.92$	$a = 0.84$	$a = 0.68$	$a = 0.36$
	Mutant allele with an adenosine-to-guanine substitution at the third nucleotide							
0.01%	- / 387	10000 / 10000	10000 / 10000	10000 / 10000	10000 / 10000	10000 / 10000	10000 / 10000	10000 / 10000
0.02%	- / 370	10000 / 10000	10000 / 10000	10000 / 10000	10000 / 10000	10000 / 10000	10000 / 10000	10000 / 10000
0.04%	- / 380	10000 / 10000	10000 / 10000	10000 / 10000	10000 / 10000	10000 / 10000	10000 / 10000	10000 / 10000
0.08%	- / 401	10000 / 10000	10000 / 10000	10000 / 10000	10000 / 10000	10000 / 10000	10000 / 10000	10000 / 10000
0.16%	- / 371	9242 / 9504	10000 / 10000	10000 / 10000	10000 / 10000	10000 / 10000	10000 / 10000	10000 / 10000
0.32%	- / 363	1932 / 3057	9304 / 9568	10000 / 10000	10000 / 10000	10000 / 10000	10000 / 10000	10000 / 10000
0.64%	- / 363	209 / 1006	1978 / 3087	9436 / 9676	10000 / 10000	10000 / 10000	10000 / 10000	10000 / 10000
1.28%	- / 401	31 / 609	234 / 1084	2224 / 3311	9616 / 9801	10000 / 10000	10000 / 10000	10000 / 10000
2.56%	- / 445	9 / 507	38 / 718	285 / 1236	2742 / 3922	9818 / 9939	10000 / 10000	10000 / 10000
5.12%	- / 1099	5 / 634	11 / 690	67 / 995	452 / 1697	3801 / 5166	9932 / 9997	10000 / 10000
10.24%	- / 3287	3 / 1158	10 / 1205	35 / 1391	117 / 1758	820 / 2856	6132 / 7503	9969 / 10000
20.48%	- / 3287	15 / 3303	27 / 3400	45 / 3565	95 / 3909	361 / 4430	2058 / 5874	8086 / 9374
	Mutant allele with a guanine inserted between the third and fourth nucleotides							
0.01%	- / 366	10000 / 10000	10000 / 10000	10000 / 10000	10000 / 10000	10000 / 10000	10000 / 10000	10000 / 10000
0.02%	- / 368	10000 / 10000	10000 / 10000	10000 / 10000	10000 / 10000	10000 / 10000	10000 / 10000	10000 / 10000
0.04%	- / 354	10000 / 10000	10000 / 10000	10000 / 10000	10000 / 10000	10000 / 10000	10000 / 10000	10000 / 10000
0.08%	- / 378	9995 / 10000	10000 / 10000	10000 / 10000	10000 / 10000	10000 / 10000	10000 / 10000	10000 / 10000
0.16%	- / 366	8604 / 8882	9998 / 10000	10000 / 10000	10000 / 10000	10000 / 10000	10000 / 10000	10000 / 10000
0.32%	- / 381	1351 / 2389	8667 / 8936	9994 / 10000	10000 / 10000	10000 / 10000	10000 / 10000	10000 / 10000
0.64%	- / 384	166 / 946	1425 / 2385	8894 / 9138	10000 / 10000	10000 / 10000	10000 / 10000	10000 / 10000
1.28%	- / 358	19 / 604	181 / 1042	1571 / 2610	9184 / 9396	10000 / 10000	10000 / 10000	10000 / 10000
2.56%	- / 424	6 / 547	21 / 698	219 / 1188	1971 / 3104	9600 / 9793	10000 / 10000	10000 / 10000
5.12%	- / 573	0 / 663	7 / 699	31 / 903	260 / 1499	2829 / 4125	9856 / 9987	10000 / 10000
10.24%	- / 1032	1 / 1079	3 / 1221	15 / 1389	79 / 1795	621 / 2765	5134 / 6494	9934 / 10000
20.48%	- / 3231	4 / 3288	6 / 3432	16 / 3553	32 / 3875	208 / 4513	1613 / 5737	7559 / 8853
	Mutant allele with a guanine-to-thymine substitution at the 37th nucleotide							
0.01%	- / 402	10000 / 10000	10000 / 10000	10000 / 10000	10000 / 10000	10000 / 10000	10000 / 10000	10000 / 10000
0.02%	- / 382	10000 / 10000	10000 / 10000	10000 / 10000	10000 / 10000	10000 / 10000	10000 / 10000	10000 / 10000
0.04%	- / 394	10000 / 10000	10000 / 10000	10000 / 10000	10000 / 10000	10000 / 10000	10000 / 10000	10000 / 10000
0.08%	- / 393	10000 / 10000	10000 / 10000	10000 / 10000	10000 / 10000	10000 / 10000	10000 / 10000	10000 / 10000
0.16%	- / 385	8867 / 8944	10000 / 10000	10000 / 10000	10000 / 10000	10000 / 10000	10000 / 10000	10000 / 10000
0.32%	- / 427	918 / 1152	9005 / 9060	10000 / 10000	10000 / 10000	10000 / 10000	10000 / 10000	10000 / 10000
0.64%	- / 392	77 / 386	855 / 1091	9050 / 9107	10000 / 10000	10000 / 10000	10000 / 10000	10000 / 10000
1.28%	- / 394	24 / 397	76 / 401	869 / 1056	9220 / 9256	10000 / 10000	10000 / 10000	10000 / 10000
2.56%	- / 452	3 / 443	13 / 429	60 / 385	868 / 1026	9480 / 9497	10000 / 10000	10000 / 10000
5.12%	- / 552	3 / 529	3 / 576	17 / 521	99 / 504	947 / 1112	9767 / 9775	10000 / 10000
10.24%	- / 1048	2 / 1058	5 / 1054	11 / 1052	43 / 1111	160 / 963	1145 / 1332	9820 / 9824
20.48%	- / 3227	8 / 3282	9 / 3461	10 / 3260	31 / 3439	99 / 3428	480 / 3043	1901 / 2481
	Mutant allele with a thymine-to-adenosine substitution at the 40th nucleotide							
0.01%	- / 367	111 / 10000	111 / 10000	95 / 10000	82 / 10000	96 / 10000	116 / 10000	97 / 10000
0.02%	- / 372	100 / 10000	112 / 10000	99 / 10000	98 / 10000	96 / 10000	126 / 10000	122 / 10000
0.04%	- / 379	110 / 10000	109 / 10000	118 / 10000	100 / 10000	117 / 10000	91 / 10000	110 / 10000
0.08%	- / 384	115 / 10000	121 / 10000	123 / 10000	99 / 10000	109 / 10000	92 / 10000	118 / 10000
0.16%	- / 379	934 / 7882	126 / 10000	111 / 10000	120 / 10000	112 / 10000	114 / 10000	103 / 10000
0.32%	- / 358	386 / 1438	921 / 7837	100 / 10000	105 / 10000	117 / 10000	88 / 10000	111 / 10000
0.64%	- / 382	99 / 566	423 / 1465	929 / 7948	106 / 10000	120 / 10000	110 / 10000	117 / 10000
1.28%	- / 401	37 / 418	105 / 541	373 / 1460	806 / 8201	96 / 10000	99 / 10000	104 / 10000
2.56%	- / 403	21 / 468	50 / 484	109 / 566	421 / 1523	663 / 8525	105 / 10000	87 / 10000
5.12%	- / 566	29 / 572	35 / 564	43 / 559	122 / 677	400 / 1592	479 / 9017	121 / 10000
10.24%	- / 1083	30 / 1100	40 / 1063	58 / 1109	81 / 1092	184 / 1182	424 / 2003	253 / 9156
20.48%	- / 3238	62 / 3344	64 / 3271	86 / 3374	102 / 3374	183 / 3520	403 / 3644	550 / 4127

Positive: the total number of simulation repeats that positively identified a mutant allele in the DNA pool.  
 True positive: the number of simulation repeats that correctly identified the mutant allele.  
 $a$  indicates the real proportion of the wild-type allele in the DNA pool.



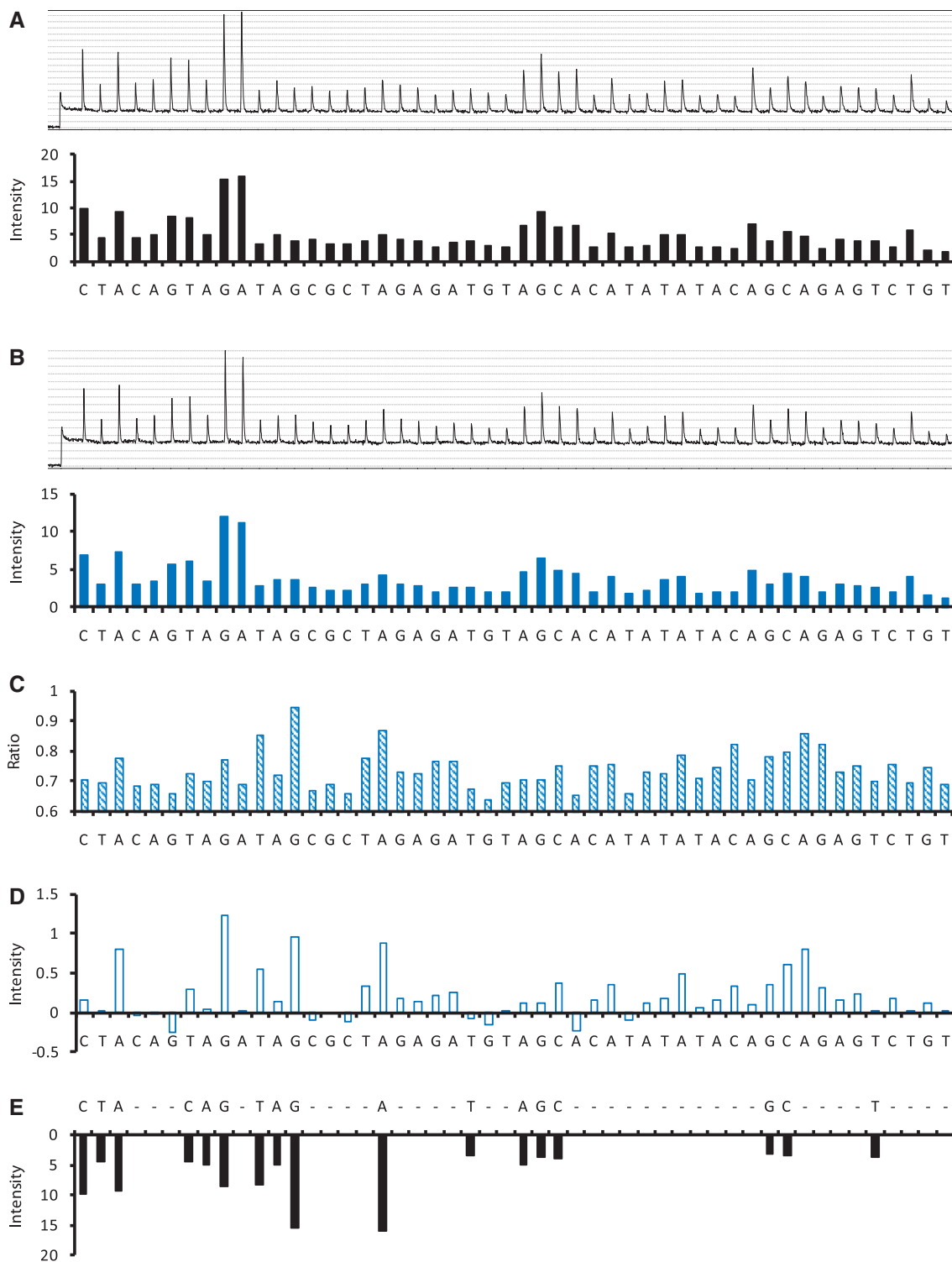


**Figure 5.** The real Pyrosequencing<sup>TM</sup> examination of the mitochondrial cytochrome *b* gene of *P. parva*: (A) the pyrogram of the wild-type DNA fragment, *W*; (B) the pyrogram of a pooled DNA sample containing 10% mutant DNA, *S*; (C) the profile *R*; (D) the profile *T*; (E) the profile *W* which is aligned to profile *T*. See the main text for the details.

29th–39th and 42nd–45th sites were supposed to have no signal being detected; however, unexpected high values (due to the signal variation) were represented on some of these sites (Figure 5D). Our dynamic programming overcame this difficulty by considering the *ad hoc* nature

of Pyrosequencing<sup>TM</sup>. We were therefore able to correctly align the profiles *T* and *W*, and predicted the sequence of the mutant allele (Figure 5D and E).

Given that the performance of our algorithm heavily depends on the level of experimental precision as

described above, it is worth to know the reproducibility of general Pyrosequencing<sup>TM</sup> reactions. Previous studies indicated that, when the same PCR products were sequenced several times, the standard deviation of the signals ranged 0.006–0.024 (32) and 0.008–0.031 (15). Doostzadeh *et al.* (22) further suggested that it is possible to reduce the values of standard deviation to 0.0003–0.0018 if the signal intensity was appropriately measured. If the coefficient of variation was limited in this range, our method could easily be used to detect rare mutant alleles (Tables 1 and 2). It should be emphasized that the purpose of our study was not to improve the quality of Pyrosequencing<sup>TM</sup> reactions and our experiments were not performed by experienced technicians. However, the result of our large-scale assay indicates that the proposed algorithm still performs well for such general Pyrosequencing<sup>TM</sup> tests (Table 3). Among all the 144 sample pairs, only one pair failed to satisfy the criteria: Shapiro–Wilk test,  $P < 0.05$ . Moreover, we accurately predicted the sequence of BY strain (the unknown allele) for 141 of the rest 143 pairs. The proportion of BY strain in the pooled DNA sample was estimated as  $12.82 \pm 3.81\%$ . We also tested the false-positive ratio using the 12 repeats with 100% RM as both wild-type sample and pooled DNA sample. In the possible 132 sample pairs, only three pairs were inaccurately predicted as with the existence of a mutant allele, i.e. W3/W6, W5/W8 and W6/W3 as the wild-type sample/the pooled sample, respectively. These examinations are consistent with our computational simulation results.

The deficiency of our algorithm is that it might fail if the pooled DNA sample contained more than one unexpected mutant allele (*de novo* SNP). Combining more than two pyrograms into one would make the derived pyrogram become too complicated to be decomposed. Fortunately, we could design a specific dispensing order of dNTPs for all the known haplotypes, and our method only has to deal with *de novo* SNPs. It is unlikely that we would frequently find two or more *de novo* SNPs in a short Pyrosequencing<sup>TM</sup> read. The other difficulty is that one haplotype might include more than one mutant

site. Modifying the scoring scheme of our dynamic programming (e.g. reducing the penalty for the second mismatch site) might help to identify some of these haplotypes. This is especially true if the mutant sites were located close to the start of the pyrogram, because sufficient signals of nonsynchronistic extensions could thus be provided to overcome the penalty of the mismatch sites. However, this kind of modifications would also increase the false-positive ratio and decrease the specificity of our prediction. Therefore, our method only focused on haplotypes with one mutant site, since mutations are supposed to be rare.

In recent years, Pyrosequencing<sup>TM</sup> has been frequently utilized to estimate the frequencies or expression levels of known alleles (13–24,26). Because the dispensing order of dNTPs was designed based on the known SNPs, the *de novo* SNPs probably used to be ignored, especially if their frequencies were not high enough to generate obvious signals of asynchronistic extensions. For this kind of studies, our method could easily be applied to examine the existence of unexpected mutant alleles in the DNA samples by comparing the obtained pyrograms. This is a simple and economical strategy for SNP genotyping surveys. On the other hand, our algorithm also has the potential to be applied for the high-throughput Pyrosequencing<sup>TM</sup> (454 platform) data. An appropriate DNA-to-bead ratio is essential for the 454 platform because only beads carrying single type of amplified templates could generate readable signals (flowgrams) (33–35). The mixed signals generated from either wells each containing multiple beads or beads each carrying multiple amplified templates are usually filtered out. In some of these cases, asynchronistic extensions may occur and our algorithm could be modified to identify these mixed DNA templates. More information could therefore be obtained. In other words, the method proposed in this study not only creates a new application for the low-throughput Pyrosequencing<sup>TM</sup> platform, but also provides a possible strategy to improve the high-throughput Pyrosequencing<sup>TM</sup> platform that might be useful in the future.

**Table 3.** The estimated proportion of BY strain (the unknown allele) in the pooled DNA samples in our large-scale Pyrosequencing<sup>TM</sup> assay

	S1	S2	S3	S4	S5	S6	S7	S8	S9	S10	S11	S12
W1	0.0954	0.1851	0.0977	0.1434	0.0916	0.1443	0.0875	0.1662	0.1045	0.1387	0.1199	0.1587
W2	0.1147	0.1387	0.1049	0.1380	0.1705	0.1417	0.1158	0.0755	0.1299	0.1026	0.1445	0.1651
W3	0.1185	0.1469	0.1480	0.1312	0.0894	0.1361	0.1623	0.1638	0.1484	0.1349	0.1130	0.1665
W4	0.1032	0.1774	0.1273	0.1281	0.1394	0.1655	0.1569	0.1593	0.1735	0.1668	0.1500	0.1456
W5	0.1252	0.1979	0.1424	0.1154	0.1980	0.1651	0.1448	0.1583	0.1451	0.1165	0.1433	0.0787
W6	0.0618	0.0412	0.0829	0.1335	0.1304	0.0330	–	0.2073	0.0708	0.2122*	0.0909	0.1078
W7	0.1084	0.1065	0.1460	0.1055	0.1099	0.1579	0.1553	0.1383	0.0756	0.1667	0.0901	0.1161
W8	0.0702	0.1562	0.1979	0.1360	0.0464	0.1264	0.1452	0.0779	0.2001	0.1095	0.0779	0.1028
W9	0.0704	0.0874	0.1002	0.1596	0.1459	0.1398	–0.0616	0.1846	0.1994	0.1871	0.1551	0.0929
W10	0.1262	0.1078	0.0904	0.1550	0.1237	0.1111	0.1274	0.0721	0.1249	0.1502*	0.0993	0.1038
W11	0.1183	0.1043	0.1240	0.1320	0.1162	0.1601	0.1049	0.1372	0.1226	0.1703	0.1256	0.1482
W12	0.1136	0.1300	0.1408	0.1078	0.0983	0.1164	0.1195	0.1472	0.1366	0.1760	0.1414	0.1352

The 12 wild-type samples (100% RM) are denoted as W1–W12, while the 12 pooled DNA samples (90% RM+10% BY) are denoted as S1–S12. The sample pair failed to satisfy the criteria: Shapiro–Wilk test,  $P < 0.05$ , is marked with (–), and the two pairs we failed to identify the correct sequence of the unknown allele are marked with (\*).

## SUPPLEMENTARY DATA

Supplementary Data are available at NAR Online.

## ACKNOWLEDGEMENTS

We thank C.-C. Chiou, J.-D. Luo, C.-H. Chang and H.-M. Sung for the assistance of Pyrosequencing™ experiments, and M.-S. Shiao and J. Rest for suggestions and help.

## FUNDING

National Science Council, Taiwan (NSC 97-2621-B-009-001 and 98-2621-B-009-001-MY3); NCTU under the grant from MoE ATU Plan. Funding for open access charge: National Science Council, Taiwan.

*Conflict of interest statement.* None declared.

## REFERENCES

- Miller, R.D., Phillips, M.S., Jo, I., Donaldson, M.A., Studebaker, J.F., Addleman, N., Alfisi, S.V., Ankener, W.M., Bhatti, H.A., Callahan, C.E. *et al.* (2005) High-density single-nucleotide polymorphism maps of the human genome. *Genomics*, **86**, 117–126.
- Frazer, K.A., Ballinger, D.G., Cox, D.R., Hinds, D.A., Stuve, L.L., Gibbs, R.A., Belmont, J.W., Boudreau, A., Hardenbol, P., Leal, S.M. *et al.* (2007) A second generation human haplotype map of over 3.1 million SNPs. *Nature*, **449**, 851–861.
- Schwarz, G., Baumler, S., Block, A., Felsenstein, F.G. and Wenzel, G. (2004) Determination of detection and quantification limits for SNP allele frequency estimation in DNA pools using real time PCR. *Nucleic Acids Res.*, **32**, e24.
- Sham, P., Bader, J.S., Craig, I., O'Donovan, M. and Owen, M. (2002) DNA Pooling: a tool for large-scale association studies. *Nat. Rev. Genet.*, **3**, 862–871.
- Risch, N. and Teng, J. (1998) The relative power of family-based and case-control designs for linkage disequilibrium studies of complex human diseases I. DNA pooling. *Genome Res.*, **8**, 1273–1288.
- Teng, J. and Risch, N. (1999) The relative power of family-based and case-control designs for linkage disequilibrium studies of complex human diseases. II. Individual genotyping. *Genome Res.*, **9**, 234–241.
- Butcher, L.M., Meaburn, E., Knight, J., Sham, P.C., Schalkwyk, L.C., Craig, I.W. and Plomin, R. (2005) SNPs, microarrays and pooled DNA: identification of four loci associated with mild mental impairment in a sample of 6000 children. *Hum. Mol. Genet.*, **14**, 1315–1325.
- Van Tassell, C.P., Smith, T.P., Matukumalli, L.K., Taylor, J.F., Schnabel, R.D., Lawley, C.T., Haudenschild, C.D., Moore, S.S., Warren, W.C. and Sonstegard, T.S. (2008) SNP discovery and allele frequency estimation by deep sequencing of reduced representation libraries. *Nat. Methods*, **5**, 247–252.
- Hyman, E.D. (1988) A new method of sequencing DNA. *Anal. Biochem.*, **174**, 423–436.
- Metzker, M.L. (2005) Emerging technologies in DNA sequencing. *Genome Res.*, **15**, 1767–1776.
- Ronaghi, M., Karamohamed, S., Pettersson, B., Uhlen, M. and Nyren, P. (1996) Real-time DNA sequencing using detection of pyrophosphate release. *Anal. Biochem.*, **242**, 84–89.
- Ronaghi, M., Uhlen, M. and Nyren, P. (1998) A sequencing method based on real-time pyrophosphate. *Science*, **281**, 363, 365.
- Wittkopp, P.J., Haerum, B.K. and Clark, A.G. (2004) Evolutionary changes in *cis* and *trans* gene regulation. *Nature*, **430**, 85–88.
- Chang, Y.-W., Liu, F.-G.R., Yu, N., Sung, H.M., Yang, P., Wang, D., Huang, C.J., Shih, M.C. and Li, W.-H. (2008) Roles of *cis*- and *trans*-changes in the regulatory evolution of genes in the gluconeogenic pathway in yeast. *Mol. Biol. Evol.*, **25**, 1863–1875.
- Ogino, S., Kawasaki, T., Brahmandam, M., Yan, L., Cantor, M., Namgyal, C., Mino-Kenudson, M., Lauwers, G.Y., Loda, M. and Fuchs, C.S. (2005) Sensitive sequencing method for KRAS mutation detection by Pyrosequencing. *J. Mol. Diagn.*, **7**, 413–421.
- Cheesman, S., Creasey, A., Degnan, K., Kooij, T., Afonso, A., Cravo, P., Carter, R. and Hunt, P. (2007) Validation of Pyrosequencing for accurate and high throughput estimation of allele frequencies in malaria parasites. *Mol. Biochem. Parasitol.*, **152**, 213–219.
- Liu, Z., Lozupone, C., Hamady, M., Bushman, F.D. and Knight, R. (2007) Short pyrosequencing reads suffice for accurate microbial community analysis. *Nucleic Acids Res.*, **35**, e120.
- Wasson, J., Skolnick, G., Love-Gregory, L. and Permutt, M.A. (2002) Assessing allele frequencies of single nucleotide polymorphisms in DNA pools by pyrosequencing technology. *Biotechniques*, **32**, 1144–1152.
- Gruber, J.D., Colligan, P.B. and Wolford, J.K. (2002) Estimation of single nucleotide polymorphism allele frequency in DNA pools by using Pyrosequencing. *Hum. Genet.*, **110**, 395–401.
- Nordfors, L., Jansson, M., Sandberg, G., Lavebratt, C., Sengul, S., Schalling, M. and Arner, P. (2002) Large-scale genotyping of single nucleotide polymorphisms by Pyrosequencing™ and validation against the 5'nuclease (Taqman®) assay. *Hum. Mutat.*, **19**, 395–401.
- Andreasson, H., Nilsson, M., Budowle, B., Frisk, S. and Allen, M. (2006) Quantification of mtDNA mixtures in forensic evidence material using pyrosequencing. *Int. J. Legal Med.*, **120**, 383–390.
- Doozadeh, J., Shokralla, S., Absalan, F., Jalili, R., Mohandessi, S., Langston, J.W., Davis, R.W., Ronaghi, M. and Gharizadeh, B. (2008) High throughput automated allele frequency estimation by pyrosequencing. *PLoS ONE*, **3**, e2693.
- Lavebratt, C., Sengul, S., Jansson, M. and Schalling, M. (2004) Pyrosequencing™-based SNP allele frequency estimation in DNA pools. *Hum. Mutat.*, **23**, 92–97.
- Neve, B., Froguel, P., Corset, L., Vaillant, E., Vatin, V. and Boutin, P. (2002) Rapid SNP allele frequency determination in genomic DNA pools by pyrosequencing. *Biotechniques*, **32**, 1138–1142.
- Mardis, E.R. (2008) The impact of next-generation sequencing technology on genetics. *Trends Genet.*, **24**, 133–141.
- Petrosino, J.F., Highlander, S., Luna, R.A., Gibbs, R.A. and Versalovic, J. (2009) Metagenomic pyrosequencing and microbial identification. *Clin. Chem.*, **55**, 856–866.
- Langae, T. and Ronaghi, M. (2005) Genetic variation analyses by Pyrosequencing. *Mutat. Res.*, **573**, 96–102.
- Pourmand, N., Elahi, E., Davis, R.W. and Ronaghi, M. (2002) Multiplex pyrosequencing. *Nucleic Acids Res.*, **30**, e31.
- Ugozoli, L.A. (2004) Multiplex assays with fluorescent microbead readout: a powerful tool for mutation detection. *Clin. Chem.*, **50**, 1963–1965.
- Zhou, G.-H., Gotou, M., Kajiyama, T. and Kambara, H. (2005) Multiplex SNP typing by bioluminescent assay coupled with terminator incorporation (BATI). *Nucleic Acids Res.*, **33**, e133.
- Shapiro, S.S. and Wilk, M.B. (1965) An analysis of variance test for normality (complete samples). *Biometrika*, **52**, 591–611.
- Dupont, J.M., Tost, J., Jammes, H. and Gut, I.G. (2004) De novo quantitative bisulfite sequencing using the pyrosequencing technology. *Anal. Biochem.*, **333**, 119–127.
- Sandberg, J., Stahl, P.L., Ahmadian, A., Bjursell, M.K. and Lundeberg, J. (2009) Flow cytometry for enrichment and titration in massively parallel DNA sequencing. *Nucleic Acids Res.*, **37**, e63.
- Zheng, Z.L., Advani, A., Melefos, O., Glavas, S., Nordstrom, H., Ye, W.M., Engstrand, L. and Andersson, A.F. (2010) Titration-free massively parallel pyrosequencing using trace amounts of starting material. *Nucleic Acids Res.*, **38**, e137.
- Metzker, M.L. (2010) Sequencing technologies – the next generation. *Nat. Rev. Genet.*, **11**, 31–46.